

Anja Schönhardt\*, A. Richter, P. Altube, K. Gerilowski, S. Krautwurst, J. P. Burrows

Institute of Environmental Physics, University of Bremen, Germany  
\*Email: schoenhardt@iup.physik.uni-bremen.de



## 1. Introduction

### Objectives of aircraft imaging DOAS measurements:

- Retrieval of tropospheric trace gases, here nitrogen dioxide NO<sub>2</sub>
- Applying Differential Optical Absorption Spectroscopy (DOAS) technique
- Mapping of NO<sub>2</sub> pollution sources, identification of source regions and strengths
- Satellite data validation, investigation of sub-pixel variability

### Positive aspects of aircraft measurements and imaging DOAS

- High spatial resolution ~100 m (down to ~30 m) at useful spatial coverage
- Several viewing directions across track are observed simultaneously
- No data gaps occur along track

### The iDOAS instrument in the Polar-5 aircraft

Aircraft Type: Basler BT-67 / DC3  
Length/Height/Span: 21 m / 5.2 m / 29 m  
Speed & Altitude: 50-105 m/s; 100-19000 ft  
Owner & Operator: AWI, Germany;  
Kenn Borek Air Ltd. Canada



Photographs: (top) iDOAS installed in Polar-5 aircraft (bottom) Polar-5 in the hangar at Bremerhaven regional airport

## 2. Instrumental setup and viewing geometry

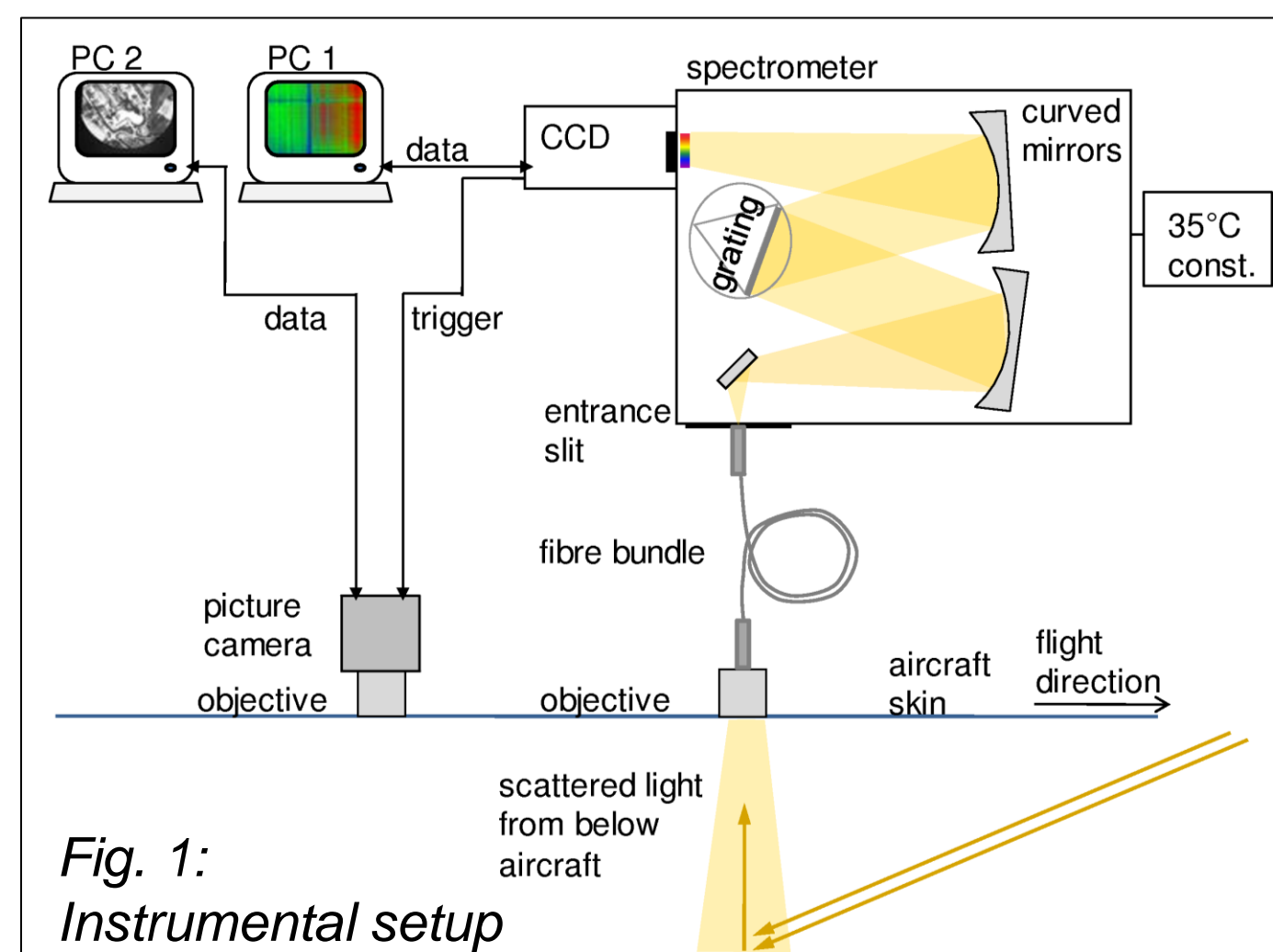


Fig. 1: Instrumental setup

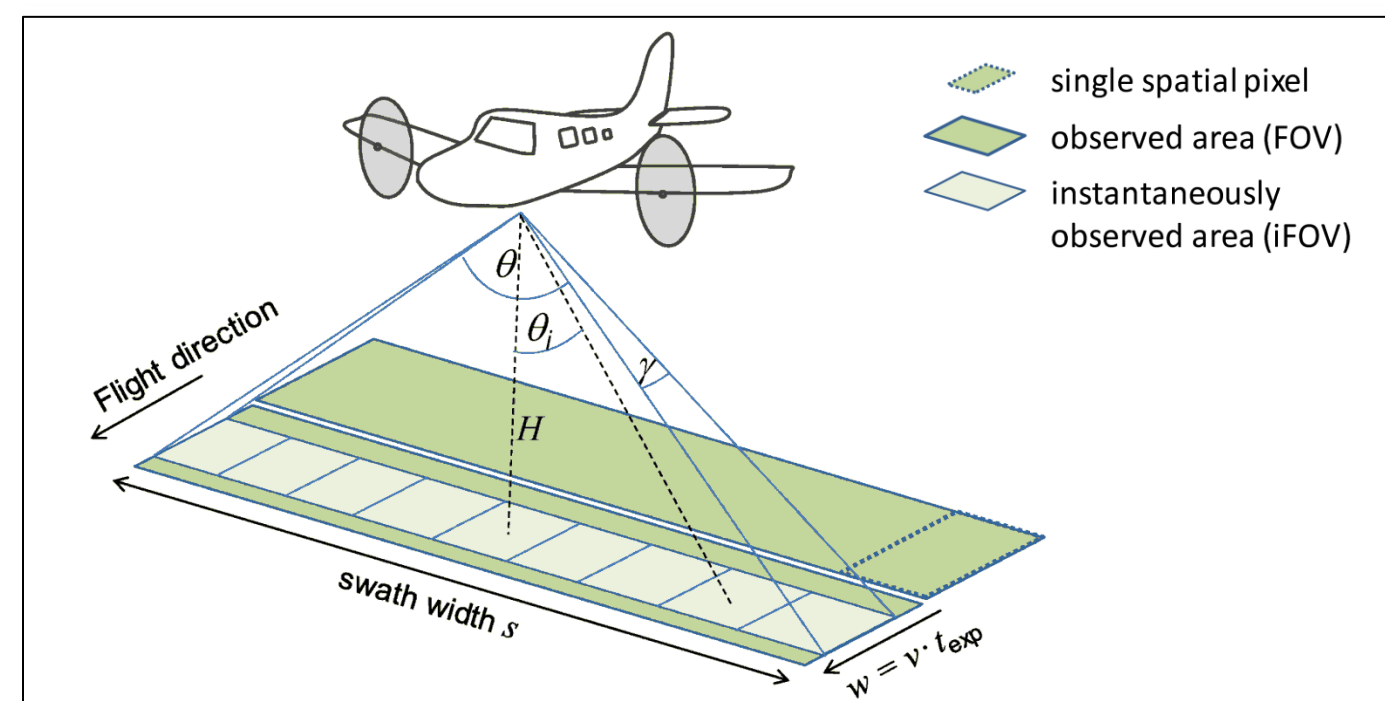


Fig. 2: The iDOAS viewing geometry

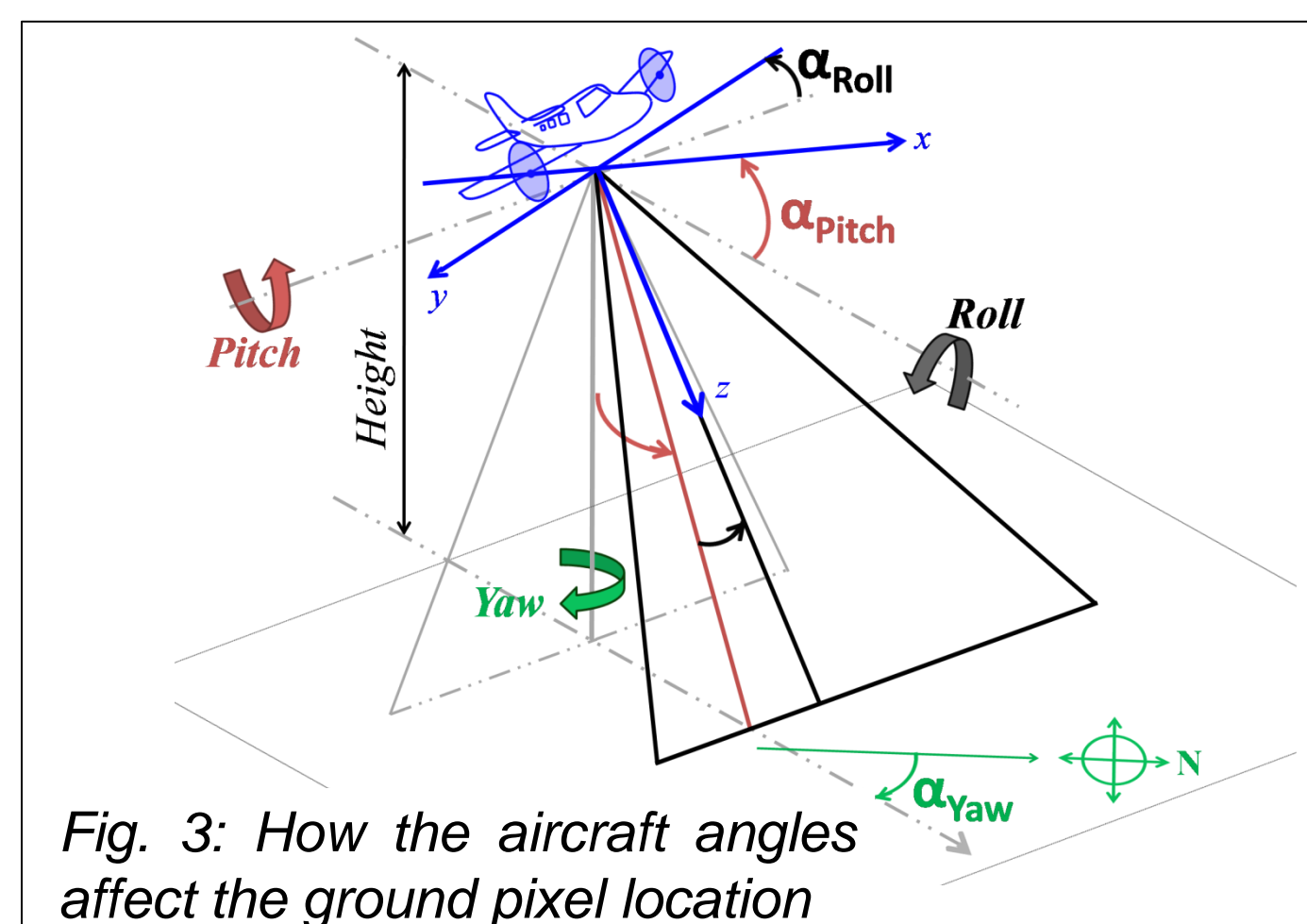


Fig. 3: How the aircraft angles affect the ground pixel location

### Technical information

- Wide angle objective and fibre bundle (35 fibres) as entrance optics
- Acton 300i imaging spectrometer
- Grating 600/mm, blazed @500nm
- Spectral window 415 - 455nm
- Spectral resolution 0.7 - 1.0nm
- Frame transfer (FT) CCD Detector, 512x512 pixels, 8.2x8.2 mm<sup>2</sup>
- Gap-free measurements (due to FT CCD) and flexible positioning in aircraft (due to sorted fibre bundle)

### Viewing geometry

- 2 nadir ports: spectrometer & camera
- Geolocation: from GPS & gyrometer
- Viewing directions: max. 35 (typ. 9) lines of sight, (LOS, θ<sub>i</sub>) from 35 fibres
- Field of view: ~48° across track (θ)
- Swath width: ~order of flight altitude H
- Exposure time t<sub>exp</sub>: typ. 0.5s
- Spatial resolution: ~100 m and less

### Computation of ground pixel location

- Consideration of the aircraft angles (pitch, roll and yaw) is required in addition to GPS position for correct determination of the geolocation
- Displacements of the ground pixel due to aircraft motions can be significant

## 3. NO<sub>2</sub> vertical columns and emission flux calculations above a power plant

### NO<sub>2</sub> retrieval above a power plant

- Black coal power plant (848 MW) at Ibbenbüren, Germany (52°17'N, 7°45'E)
- Slant columns of NO<sub>2</sub> retrieved by Differential Optical Absorption Spectroscopy
- Large variability of NO<sub>2</sub> amounts across and along track is observed
- The NO<sub>2</sub> in the exhaust plume downwind of the power plant is clearly visible
- Transects through the plume are used for emission flux estimations

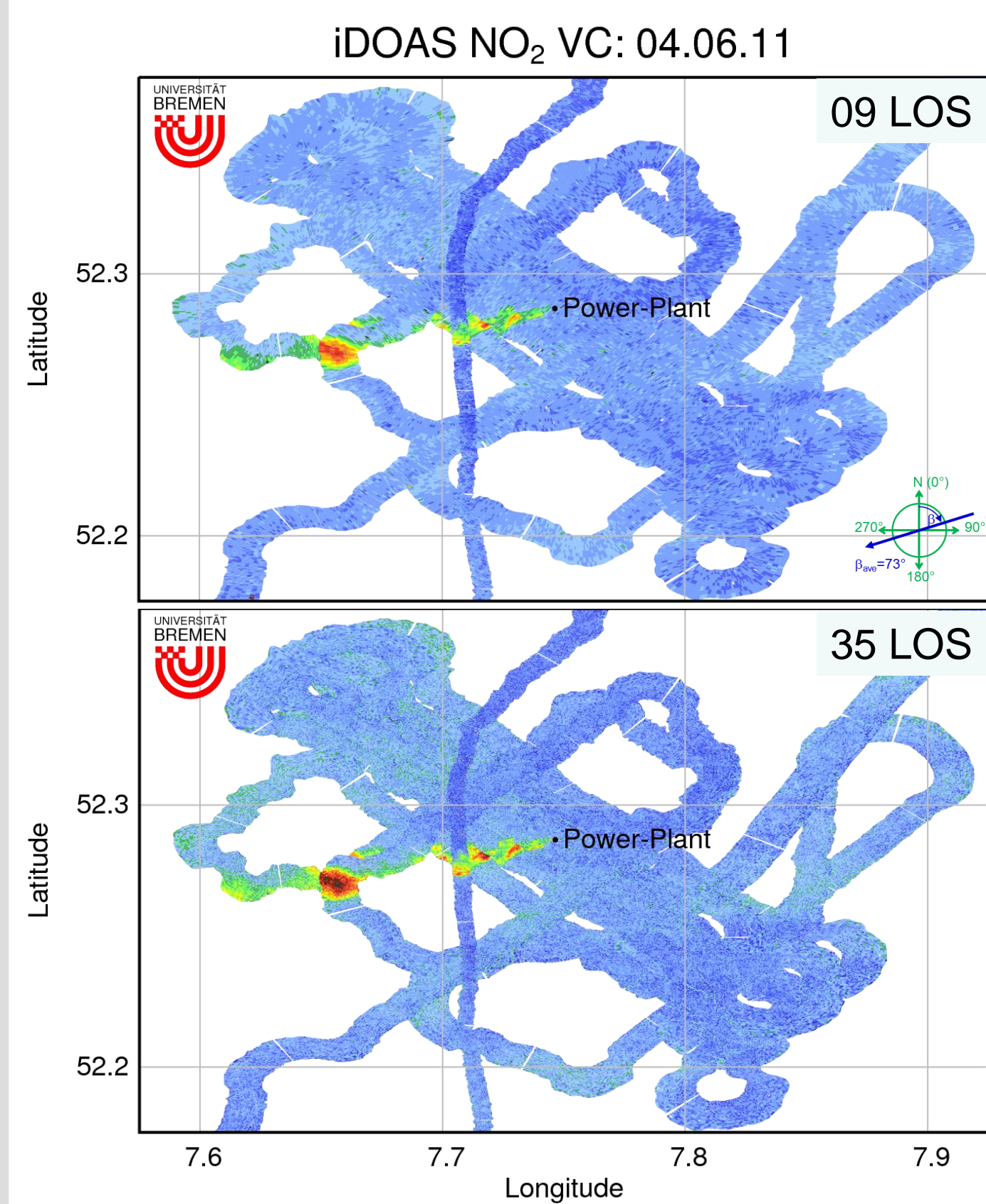


Fig. 4: NO<sub>2</sub> vertical column amounts along the flight track retrieved from the flight on 04.06.2011. Downwind from the power plant of Ibbenbüren, strong enhancement of NO<sub>2</sub> is visible. Average wind direction was about East North-East, see inset. Enhanced NO<sub>2</sub> is on the order of 10<sup>16</sup> molec/cm<sup>2</sup> with maxima > 2 · 10<sup>16</sup> molec/cm<sup>2</sup>. Top: Division of the field of view into 9 lines of sight (LOS) allowing spatial resolution of ~100m. Bottom: Consistent result for full spatial resolution of 35 LOS with ground pixel side length on the order of around 30m. Fine spatial variability of NO<sub>2</sub> amounts is resolved.

### Retrieval Settings

**Fitting window:** 425 – 450 nm  
**Trace gases:** NO<sub>2</sub> (293K), O<sub>3</sub> (241K), O<sub>4</sub> (296K), H<sub>2</sub>O (HITRAN)  
**Atmospheric effects:** Ring (SCIATRAN calculated), intensity offset  
**Polynomial:** quadratic  
**Reference I<sub>0</sub>:** rural scene from same LOS  
**Slit function:** individual for each LOS  
**Detection Limit for NO<sub>2</sub>**  
Slant Column (SC) detection limit: ~10<sup>15</sup> molec/cm<sup>2</sup>  
Optical density RMS: on the order of 10<sup>-3</sup> for a single measurement of 0.5s and an individual LOS.  
**Air mass factors, AMF (SCIATRAN calculations)**  
Rayleigh atmosphere, 1 km NO<sub>2</sub> box profile, 5% albedo, SZA and LOS dependence.

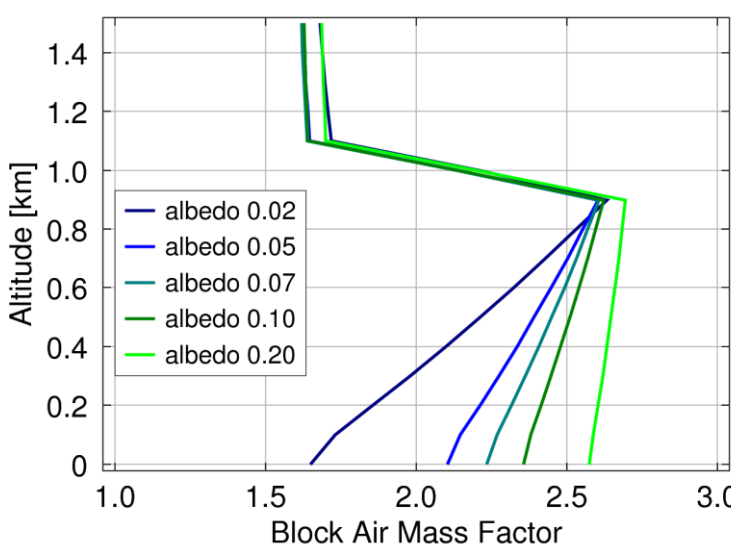
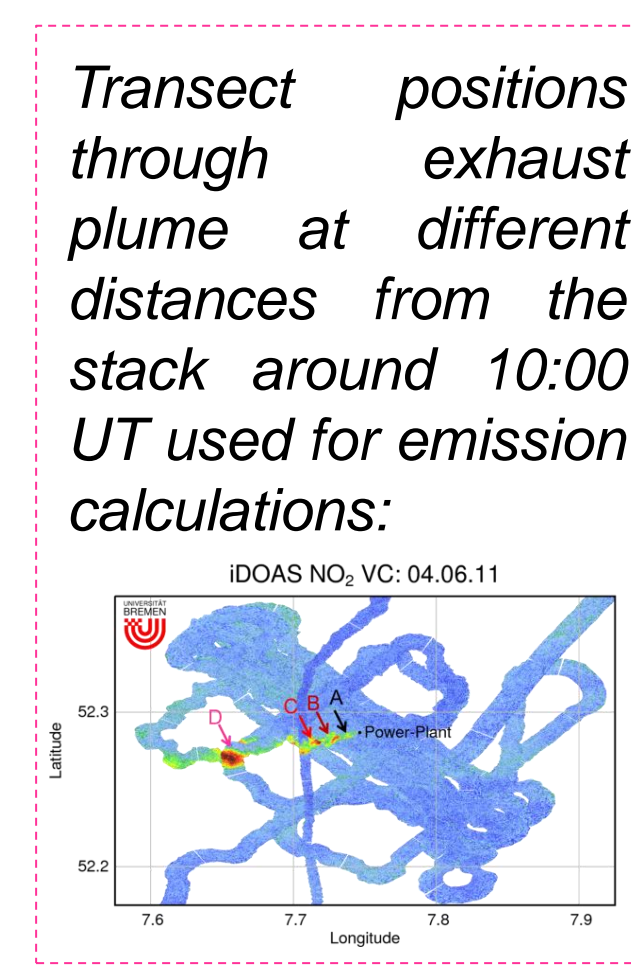


Fig. 5: Block AMF for different albedos at 40° SZA and 1.1km flight altitude. AMF differences between box profile and elevated Gaussian plume are ~10%.



### NO<sub>2</sub> emission flux calculations

- Based on Gaussian plume dispersion model
- Mean wind speed & direction determined using COSMO-DE model wind data and weighting by NO<sub>2</sub> profile (Gaussian shape, cp. Fig.6)
- Flux calculations performed at different distances from stack

$$c(x, y, z) = \frac{Q}{2\pi\sigma_y\sigma_z u} \exp\left(-\frac{y^2}{2\sigma_y^2}\right) \exp\left(-\frac{z^2}{2\sigma_z^2}\right) \quad \text{Eq. 1: Gaussian distribution of concentration } c$$

Dispersion of concentration  $c$  across plume ( $y$ ) and over altitude ( $z$ ) is taken into account, with source strength  $Q$ , wind speed  $u$  and spread  $\sigma_y$  and  $\sigma_z$ . Along the wind direction  $x$  only advection is considered.

$$Q \cong \int_L VC \cdot \vec{u} \cdot d\vec{l} \approx \sum_i VC_i \cdot \vec{u} \cdot d\vec{l}_i \quad \text{Eq. 2: Derived using Gaussian divergence theorem}$$

Approximation of source strength is achieved via discrete sum over product of vertical columns (VC), wind speed and path length  $d\vec{l}$ .

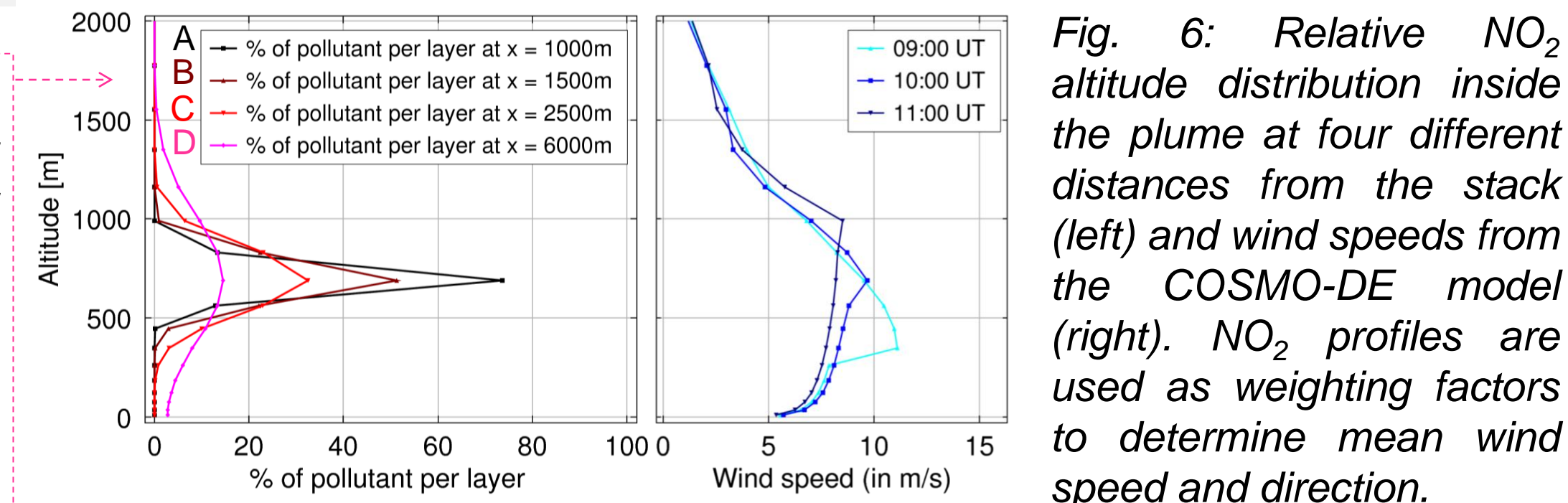


Fig. 6: Relative NO<sub>2</sub> altitude distribution inside the plume at four different distances from the stack (left) and wind speeds from the COSMO-DE model (right). NO<sub>2</sub> profiles are used as weighting factors to determine mean wind speed and direction.  
→ Estimated NO<sub>2</sub> emissions: Q<sub>NO<sub>2</sub></sub> ≈ 2100-2400 T/a  
→ Emissions of NO<sub>x</sub> (using NO/NO<sub>2</sub> ≈ 1/4): Q<sub>NO<sub>x</sub></sub> ≈ 2600-3000 T/a  
→ Results are in agreement with E-PRTR\*

## 4. NO<sub>2</sub> above inhabited and rural areas

### NO<sub>2</sub> above Hamburg and Northern Germany

- Urban NO<sub>2</sub> SC maxima lie around 1 · 10<sup>16</sup> molec/cm<sup>2</sup>
- Enhanced NO<sub>2</sub> above Hamburg and close to the airport
- Strong spatial variability of NO<sub>2</sub> is observed



Fig. 7 (left): NO<sub>2</sub> observations during two overflights over the city of Hamburg (same colour scale as Figs. 4 & 9). The flight altitude determines the width of the swath.

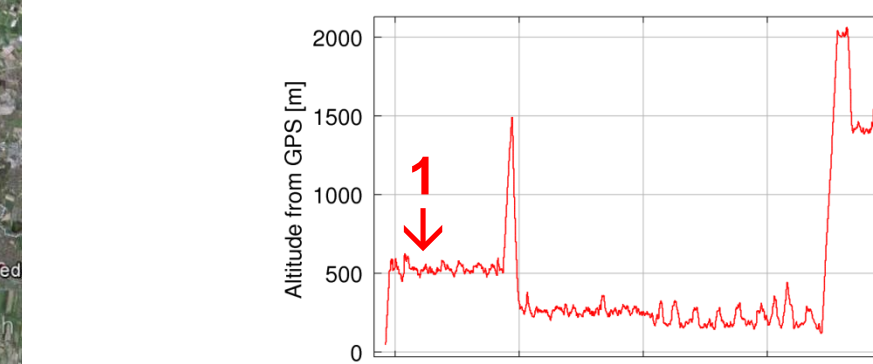


Fig. 8: Flight altitude on 09.06.2011

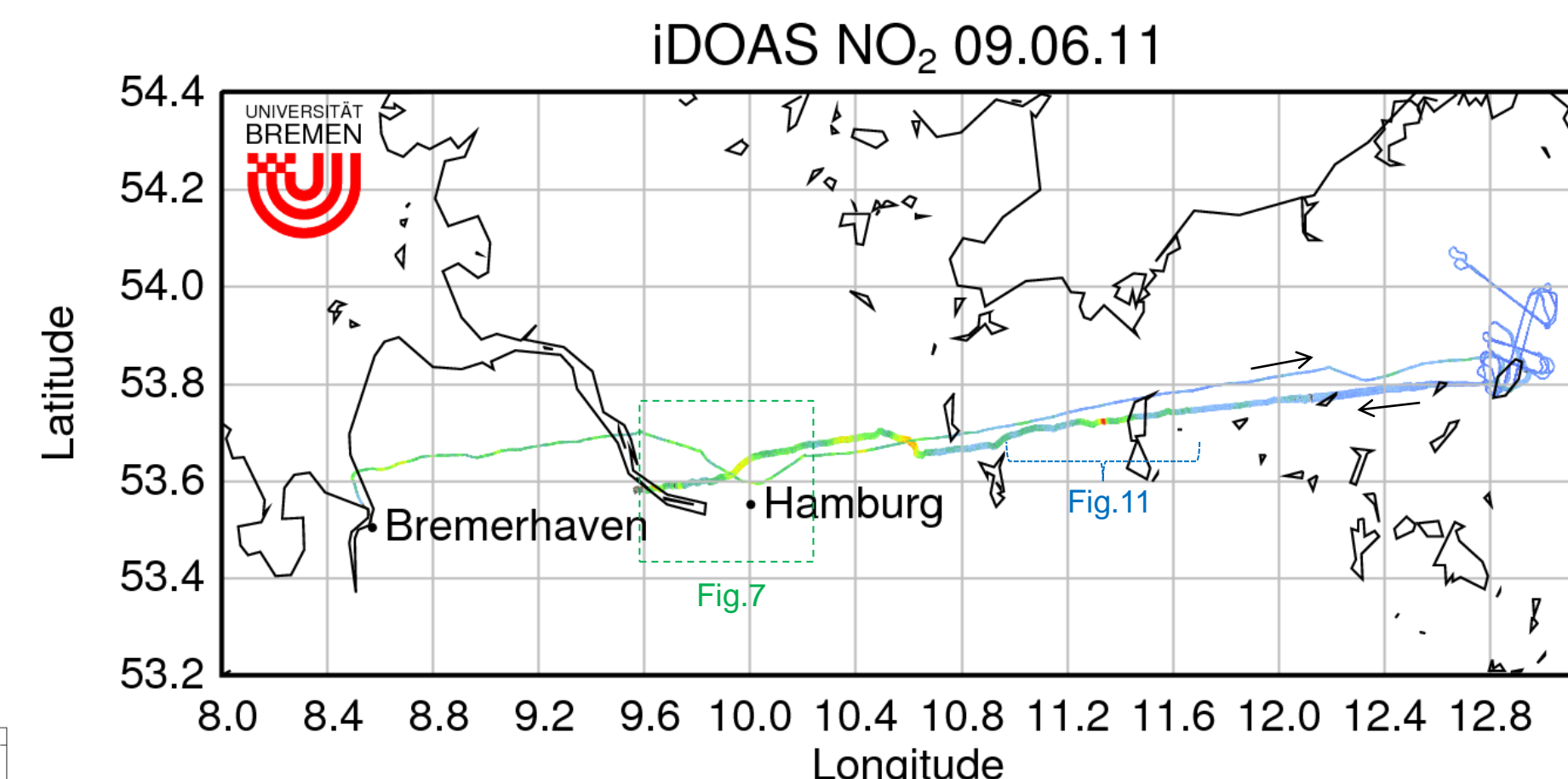


Fig. 9: NO<sub>2</sub> vertical columns observed on 09.06.2011. Strong differences in NO<sub>2</sub> results are seen: much smaller amounts above rural areas, e.g. for the East part of the flight track, than closer to cities, e.g. around the Hamburg area. Not all NO<sub>2</sub> enhancements can be directly assigned to local sources, also transported NO<sub>2</sub> is observed. Green box: Region shown in Fig. 7. Blue bracket: Section shown in Fig. 11 with confined NO<sub>2</sub> enhancement.

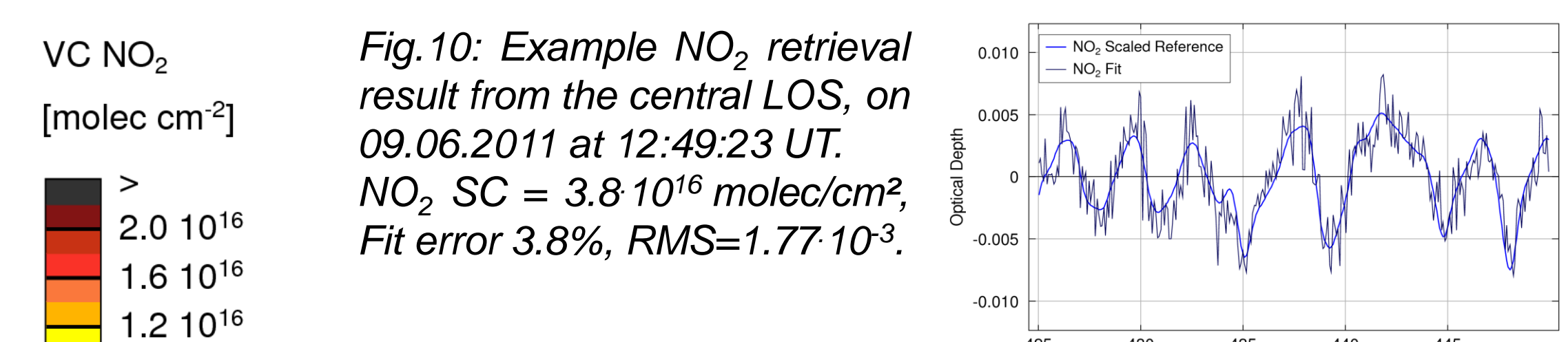


Fig. 10: Example NO<sub>2</sub> retrieval result from the central LOS, on 09.06.2011 at 12:49:23 UT. NO<sub>2</sub> SC = 3.8 · 10<sup>16</sup> molec/cm<sup>2</sup>, Fit error 3.8%, RMS=1.77 · 10<sup>-3</sup>.

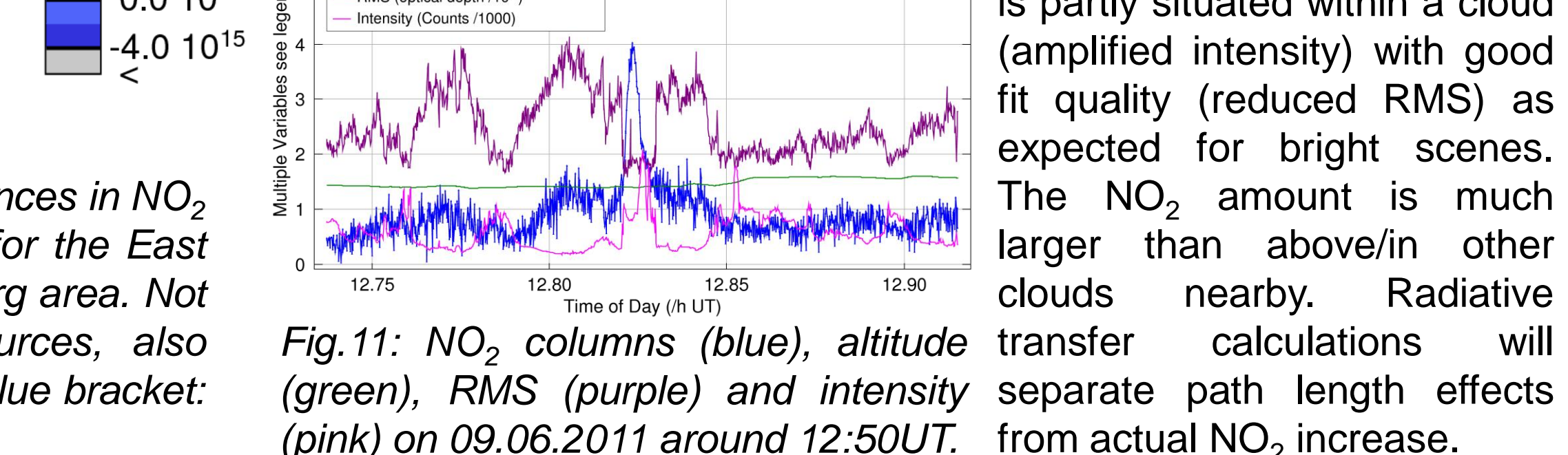


Fig. 11: NO<sub>2</sub> columns (blue), altitude (green), RMS (purple) and intensity (pink) on 09.06.2011 around 12:50 UT. NO<sub>2</sub> enhancement at 12.82UT is partly situated within a cloud (amplified intensity) with good fit quality (reduced RMS) as expected for bright scenes. The NO<sub>2</sub> amount is much larger than above/in other clouds nearby. Radiative transfer calculations will separate path length effects from actual NO<sub>2</sub> increase.

## 5. Summary & Outlook

### Summary

- Imaging DOAS instrument shows good imaging quality and good performance for NO<sub>2</sub> measurements
- Aircraft pitch, roll and yaw angles are fully taken into account for correct ground geolocation
- NO<sub>2</sub> column amounts have been retrieved, pollution sources are observed (power plant, cities, etc)
- Further findings: Large spatial NO<sub>2</sub> variability, consistent NO<sub>2</sub> retrieval results for different LOS divisions, transported NO<sub>2</sub> within a cloud away from local sources, consistently low NO<sub>2</sub> above rural areas
- NO<sub>2</sub> emission fluxes are calculated for a power plant point source in agreement with emission reports

### Activities for the future

- Air mass factor consideration will be refined in future analyses
- Further dedicated campaigns will be conducted with the imaging DOAS instrument above pollution sources

### Acknowledgements

The presented work is financially supported by the University of Bremen. Campaign support from AWI Bremerhaven, Martin Gehrmann and Franziska Nehring, is gratefully acknowledged. Thank you to the aircraft crew from Kenn Borek, Canada. COSMO-DE model data is provided by the German weather service DWD. Radiative transfer calculations are performed with the IUP Bremen SCIATRAN model, thanks to V. Rozanov.

### Selected References

- P. Wang, et al: Measurements of tropospheric NO<sub>2</sub> with an airborne multi-axis DOAS instrument, Atmos. Chem. Phys., 5, 337–343, 2005.
- F. Lohberger, et al : Ground-based imaging differential optical absorption spectroscopy of atmospheric gases, Vol. 43, No. 24, Applied Optics, 2005.
- K.-P. Heue, et al : Direct observation of two dimensional trace gas distributions with an airborne Imaging DOAS instrument, Atmos. Chem. Phys., 8, 6707–6717, 2008.
- C. Popp et al.: High-resolution NO<sub>2</sub> remote sensing from the Airborne Prism Experiment (APEX) imaging spectrometer, Atmos. Meas. Tech., 5, 2211–2225, 2012.